Automotive Experiences
Vol. 6 No. 1 (2023) pp. 23-37
p-ISSN: 2615-6202 e-ISSN: 2615-6636

Research Paper

Performance of Adsorbent from Calcium Carbide Residue to Reduce Exhaust Emissions of Two-wheeler

Hendry Sakke Tira[1], **Made Wirawan**[1], **Samsul Rahman**[1], **Ekarong Sukjit**[2], **Sudirman**[3]

[1]Department of Mechanical Engineering, University of Mataram, Mataram 83125, Indonesia
[2]School of Mechanical Engineering, Institute of Engineering, Suranaree University of Technology, Nakhon Ratchasima, 30000, Thailand
[3]Department of Chemistry, University of Mataram, Mataram 83125, Indonesia

hendrytira@unram.ac.id

https://doi.org/10.31603/ae.7827

Check for updates

Published by Automotive Laboratory of Universitas Muhammadiyah Magelang collaboration with Association of Indonesian Vocational Educators (AIVE)

Article Info
Submitted:
06/09/2022
Revised:
17/11/2022
Accepted:
03/12/2022
Online first:
21/01/2023

Abstract

The performance of calcium carbide residue in reducing two-wheel exhaust emissions has been studied. To perform this experiment, the carbide residue was first converted into adsorbent and then mounted in the exhaust gas line. Two-wheeler used are vehicles commonly used among Indonesian motorcyclists. The test was carried out by varying the adsorbent dimensions and engine transmission. Engine emission tests and adsorbent performance investigations were performed both before and after the exhaust emissions made contact with the adsorbent. The results showed that upon direct contact with the carbide adsorbent, the emission of two-wheeled engines decreased. Carbon-based emissions were reduced significantly in the early stages of the experiment. Moreover, emissions reduction benefits are seen in all adsorbent and transmission engine configurations. The greater the adsorbent's surface area, the better the emission reduction. A significant emissions reduction is also achieved when the first engine transmission condition is applied compared to the neutral transmission. However, the adsorption efficacy declined over time in all research variations. The presence of channels and pores in the adsorbent, and the high temperature attained by the adsorbent, keep improving the adsorbent's adsorption capabilities. However, as saturation increases, the adsorbent's adsorption, and oxidation capability decline.

Keywords: Calcium carbide; Adsorbent; Emissions; Two-wheeler

1. Introduction

Solid waste is currently an important concern in many countries. Problems arise when the amount of waste produced increases. As a result, solutions are needed to deal with the waste, such as providing adequate landfill sites. Problems occur if the handling of solid waste does not run optimally because it will have an impact on decreasing the quality of the environment and public health. Therefore, efforts and strategies for conservation and recycling of solid waste are needed to save the environment and protect health [1]–[3]. This development also needs to pay attention to the economic aspect. Increasing raw material costs, environmental concerns, and depletion of natural resources have all contributed to an increase in demand for alternative wastes, and therefore for materials that may be utilized as emission-reducing adsorbers in vehicles. Calcium carbide is one of the solid wastes that has received attention for its potential to be employed and empowered [4].

Calcium carbide residue (CCR) is a leftover product formed when calcium carbide (CaC_2) is hydrolyzed in the production of acetylene gas (C_2H_2). When calcium carbide reacts with water, acetylene and CCR are produced. CCR is an aqueous slurry that contains >80% calcium hydroxide ($Ca(OH)_2$), 10% calcium carbonate ($CaCO_3$), and minor silicates and carbon [5],. The

reaction mechanism can be described using the Eq. (1) [6]:

$$CaC_{2(s)} + 2H_2O_{(l)} \rightarrow C_2H_{2(g)} + Ca(OH)_{2(s)} \quad (1)$$

It is possible to convert 64 grams of calcium carbide into 74 grams of CCR ($Ca(OH)_2$) and 26 grams of acetylene gas (C_2H_2), as shown in Eq. (1). The excess alkalinity of the CCR causes a plethora of environmental issues when it is disposed of in landfill.

In other research, CCR has been tested as a filler for hot mix asphalt (HMA). The results show that CCR has great potential if its chemical and physical characteristics are in accordance with applicable regulations. They discovered that HMA with CCR had superior high temperature resistance than mixes with limestone fillers [7].

Other applications of the use of CCR have also been carried out in a test for example as a calcium promoter to improve strength development. The positive results obtained were mainly due to the high content of calcium hydroxide ($Ca(OH)_2$) in CCR [8]. This great strength is derived from the reaction of SiO_2 and Al_2O_3 from high-calcium with $Ca(OH)_2$ contained in CCR [9]. As a result of these benefits, CCR can be utilized as an addition in the cement making process.

The effectiveness of calcium carbide is also proven in the process of separating components from rubber industrial waste such as iron, zinc and heavy metals. As a result, the turbidity level of the effluent can be minimized. Rubber wastewater treatment can provide permeate that passes quality standards, allowing it to be reused as residential water for industrial water applications [10].

Lei Wu has investigated the effects of various surfactants and solid particles on foamed calcium carbide slag. The calcium carbide slag foam has been reported to efficiently suppress CO_2 mineralization and coal spontaneous combustion. Calcium carbide slag foam is expected to be used in the coal mining process to avoid accidents in gob areas and store massive amounts of CO_2 [11].

Wenfeng Li et al. studied the performance of calcium carbide in the desulfurization of diesel oil. Six alkyl carbon (ACM) compounds were produced through the mechanochemical reaction of calcium carbide with different polyhalo-hydrocarbons. According to the findings, ACM exhibited an excellent adsorption performance and selectivity, stable fixation and adsorptive characteristics [12].

As an effort to reduce vehicle emissions, carbon-based materials can be an option used as an adsorbent. This material is chosen because of its high porosity, high specific surface area, and ability to remove inorganic and organic compounds. The performance of the adsorbent can be classified into several mechanisms, including surface chemical reaction (which includes surface complexation and ion exchange) and diffusion. Furthermore, the adsorption mechanism model that occurs is highly dependent on the adsorbate and the quality of the adsorbent obtained during the preparation stage [13].

Moreover, in order to obtain a good adsorption capacity, several important factors must be considered before the adsorbent is used, including a large porous network to optimize the diffusion process, a large surface area to attract adsorbate molecules, the pore size of the adsorbent must be able to facilitate the diameter of the adsorbate molecules, and micropore volume capable of adsorbing high adsorbate capacities. Carbon-based adsorbents are relatively inexpensive because the raw material sources can include agricultural by-products and waste materials. In addition, another advantageous factor is that raw materials are easy to obtain because in current developments all low-cost materials containing carbon can be used as raw materials for carbon-based adsorbents. Even though it is cheap and easy to obtain, its adsorptive capacity performance is also very good so that it is widely applied both for emissions or areas of environmental clean-up and handling waste-waters [14]. They are also a versatile sort that can be customized. Activated carbon (AC) carbon airgel, activated carbon fiber (ACF), carbon nanotubes (CNT), fullerenes, and graphene can all be formed depending on the starting material and synthesis procedure [12], [15].

Apart from carbon-based adsorbent, CCR also has good potential as an adsorbent raw material. This is supported by the ease of obtaining raw materials and low prices. In addition, some literature states that calcium-based adsorbents can capture CO_2, one of the most dangerous greenhouse gas emissions [13].

Furthermore, the continued growth in the number of two-wheeler is accompanied by an increase in hazardous emissions emitted into the environment. Both the environment and humans are at risk from these pollutants. Therefore, after-treatment methods are required to reduce these negative consequences. There are several after-treatment technologies that can be applied to reduce engine emissions as shown in the **Table 1**.

Unfortunately, the present approach in reducing emissions from two-wheeled vehicles is the before-treatment method [16], [17]. On the other hand, discussion regarding the application of after-treatment on two-wheeled vehicle is rarely explored in the literature. Thakur Mukesh did an investigation on the two-wheeler. The research conducted a study with two-wheeler employing copper nanoparticles as a catalytic converter. The findings reveal that when the nanoparticle size decreases, the emission level decreases. Furthermore, the employed adsorbent is heat resistant, which the catalytic converter requires [18].

However, it is hard to trace study paper uses CCR as an adsorbent material on two-wheeler. On the other hand, CCR has properties that support its role as an adsorbent. The potential of CCR as an adsorbent for exhaust gas emissions can be estimated from the main composition in the form of calcium hydroxide ($Ca(OH)_2$) or in the form of Calcium oxide (CaO). When subjected to a heating process the component has a strong affinity for CO_2, CO and CHO. Therefore, a study has developed CaO-based adsorbents to capture carbon components. In addition, naturally, the CaO formed a cubic nanocrystal structure with a size of 18.61-45.03 nm and a specific surface area of 24.32-50.73 m^2/g which is suitable for attracting certain gases from vehicles. However, CaO-based adsorbents are generally obtained through synthesis [19].

This study was conducted based on the good results of prior studies that demonstrated numerous advantages of calcium carbide residue. Although the previous application was for different objectives, it is envisaged that the benefits of calcium carbide residue can also be applied to two-wheeler. Therefore, the purpose of this research was to investigate into the ability of calcium carbide to perform as an emission adsorption material in the exhaust emissions of two-wheeler.

2. Methods

2.1. Engine specification

To perform the test, two-wheeler with the engine specifications shown in **Table 2** are employed. The two-wheeler is a single-cylinder spark-ignition engine. The exhaust system was adjusted in order to facilitate engine emissions measurement. To allow the installation of the calcium carbide adsorbent, the original exhaust pipe was replaced with a customized muffler (**Figure 1**). Furthermore, the test was performed on three distinct adsorbent sizes, notably 50, 100, and 150 mm with a diameter of 88 cm. A number of thermocouple-compatible holes are provided in both the adsorbent and the exhaust gases emission pipe for temperature and pressure measurement. Three temperature measurement points are located in front of the adsorbent and one after the adsorbent. The temperature measurement is positioned inside the adsorbent at a single location under a length of 50 mm. Meanwhile, for temperature measurements, 100 and 150 mm adsorbent lengths were deployed in two and three locations, respectively. The ambient temperature and pressure were also monitored during the test.

Table 1. After-treatment technology for emissions reduction

No	Technology	Impact on Emission
1	DOC (Diesel oxidation catalyst)	CO and HC emissions were significantly reduced, PM (Particulate Matter) decreased but small to moderate, improving SCR and DPF performance [20]
2	Urea + SCR (selective catalytic reduction) catalyst	NOx reduced by 90%, meets Euro V requirements [21]
3	DPF (Diesel particulate filter)	PM reduced by up to 90%, meets Euro VI requirements [22]
4	Oxidation catalyst	CO and HC reduced by up to 90%, used in SI engines [23]
5	Three-way catalyst	CO, HC and PM reduced by up to 90%, used in most SI engines [24]
6	Particle oxidation catalyst	PM reduced by up to 50%, used in heavy-duty truck engines [25]
7	NOx adsorber catalyst	NOx reduced by 70-90%, meets Euro V requirements [26]
8	GPF (Gasoline Particulate Filters)	PM reduced to 90%, used in GDI engines, meets Euro VI requirements [27]

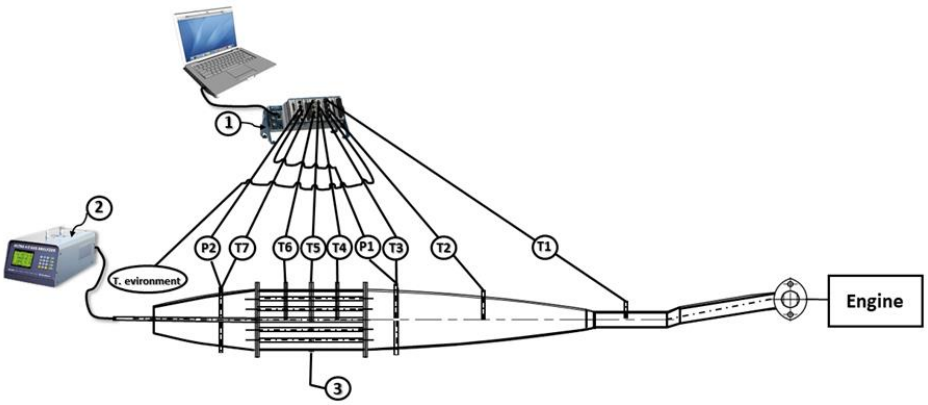

Figure 1. Schematic diagram of experimental systems (1. National Instrument Data acquisition, 2. Hanatech gas analyzer, 3. Adsorbent casing, T1-T7 temperature measurement points, P1-P2 pressure measurement points)

Table 2. Engine spesification

Engine specification		Data
Engine type	:	Single overhead camshaft
Engine cycle	:	4-stroke
Bore/stroke	:	50 x 49.5 mm
Displacement volume	:	97.1 cm^3
Compression ratio	:	9.0 : 1
Rated power	:	7.3 PS @ 8,000 rpm
Peak torque	:	0.74 kgf.m @ 6,000 rpm
Gear settings	:	N-1-2-3-4-N (rotary)

2.2. *Instruments*

K-type thermocouples are used to measure all temperatures. Before use, the thermocouple was calibrated in an oil bath with an accuracy of ±0.5 ^oC against the RTD (Resistance Temperature Detector) 100 probe calibrator. The oil bath was constructed using a pan, a 1500 W heater, and a PID (Proportional-Integral-Derivative) controller. The temperature and pressure data were recorded using NI DAQ9178 interfaced with laptop using the LabView program.

Exhaust gas pressure before and after adsorbent is also measured by mounting a pair of pressure gauges. A pair of gauge pressure sensors for gas with a maximum pressure of 250 psi were employed. The accuracy and response time of the apparatus are 2% and 1 ms, respectively. The measurement was performed to assess the pressure difference induced by the presence of the adsorbent, as well as the influence that may be triggered by the accumulation of engine emissions in the adsorbent. Temperature and pressure profiles are monitored in real time throughout testing. Apart from the exhaust emission pipe, no other adjustments to the engine were performed.

A Hanatech IM 2400 ULTRA 4/5 gas analyzer was used to measure engine emissions. Emission data is retrieved once the engine oil temperature is constant. The engine emissions measured are HC, CO, and CO_2. Following the emission test, the adsorbent in contact with the exhaust gas was submitted to SEM (Scanning Electron Microscope) and EDX (Energy Disperse X-Ray) tests. The JEOL JSM-6510LA is used for this purpose, and SEM testing is integrated with EDX. The purpose of this experiment is to determine the surface morphology and abundance of element and component. In addition, FT-IR studies were also performed to investigate changing of atomic interaction. X-Ray Diffraction testing was conducted to determine the physical characteristic of the CCR used. All of these experiments were performed to obtain an accurate picture of the adsorbent's potential to adsorb hazardous gas emissions.

The engine speed operating conditions are 1400 rpm both at idle and first engine transmission. During the test, the engine speed is kept constant and measured with a digital tachometer.

The data on engine emissions was recorded three times. The recording duration for each emission data is approximately 30 seconds, therefore the overall time spent on data collection is not thought to have a substantial impact on adsorbent saturation. As a result, the data acquired at each stage is thought to be unaffected by adsorbent saturation, suggesting that all data is affected by the same variables. Furthermore, testing was performed to determine the saturation limit of the adsorbent. This was accomplished by running the test for four hours.

2.3. Adsorbent Preparation

The typical material of adsorbent in this study was obtained from the welding household industry in the form of a white slurry which is a residue from the use of calcium carbide as a precursor of acetylene gas, hence known as CCR. The slurry is first sieved to obtain uniform size and remove any unwanted particles. The material is then mixed with water in a ratio of 7:1. The mixture is then manually stirred until it is evenly distributed. After that, the mixture is placed in a mold that has been prepared to a predetermined dimension. Each adsorbent had 19 pores with a diameter of 6 mm. The mold was then left at room temperature for 24 hours. Until this stage, the manufactured adsorbent has a fairly good hardness. The adsorbent is then heated in a furnace at 200 °C for four hours. This is done to ensure that the water content in the adsorbent is removed. Changes in the characteristics of the adsorbent before and after contact with the exhaust gas were studied with the Fourier Transform Infrared instrument, X-Ray Diffraction, Scanning Electron Microscopy and Energy Disperse X-Ray spectroscopy.

2.4. Fuels

The fuel used in this experiment was obtained from PT Pertamina, an Indonesian national oil company. The characteristics of the fuel used are presented in **Table 3**.

3. Results and Discussion

3.1. Effect of Adsorbent Dimension on Exhaust Emissions

Carbon monoxide (CO) gas emissions result from incomplete combustion. Carbon monoxide is a relatively unstable gas that reacts with numerous substances. Another feature is that it can be converted easily into CO_2 with a little oxygen and heat. The concentration level of the remaining combustion products is heavily determined by the ratio of fuel and air inhaled by the engine. The more appropriate the ratio of the fuel to air mixture, the lower the CO emissions produced. Furthermore, in order to reduce CO, the mixture's ratio must be made lean [28].

Meanwhile, hydrocarbon (HC) emissions occur as a result of incomplete combustion, which results in the fuel not being involved in the com-

Table 3. Physical and chemical data of Pertamina gasoline [29]

Characteristics	Unit	Range		Test method
		Without lead		
		min	max	ASTM
1. Octane number				
RON	RON	88.0		D 2699-86
MON		reported	reported	D 2700-86
2. Oxide stability	minute	360	-	D 525-99
3. Sulfur content	% mm	-	0.05	D 2622-98
4. Pb content	gr/l	-	0.013	D 3237-97
5. Distillation				D 86-99a
10% evaporation vol.	°C	-	74	
50% evaporation vol.	°C	88	125	
90% evaporation vol.	°C	-	180	
Final boiling point	°C	-	215	
Residue	% vol	-	2.0	
6. Oxygen content	% m/m	-	2.72	D 4815-94a
7. Washed gum	mg/100 ml	-	5	D 381-99
8. Vapor pressure	kPa	-	62	D 5191/D 323
9. Density at 15 °C	kg/m³	715	780	D 4052/D 1298
10. Copper blade corrosion	minute	First class		D-130-94
11. Doctor test		Negative		
12. Mercaptan sulfur	% mass	-	0.002	D-3227
13. Visual appearance		Clear and bright		
14. Color		Red		
15. Coloring content	gr/100 l	0.13		
16. Odor		marketable		

bustion process. Any unburned fuel is expelled as a hydrocarbon chain together with other combustion gases during the exhaust stroke [30]. The results of the engine emission are shown in **Figure 2**. It is noted that there is a decrease in the concentration of all exhaust gas emissions, both in the operating conditions of neutral transmission and also transmission 1 after the application of the adsorbent unit. However, the small decrease in CO is most likely due to CO has a high electronegativity, while the composition of the adsorbent is dominated by base oxide components (CaO, and Al_2O_3). This makes it difficult for the adsorbent to attract CO. The possible mechanism of CO oxidation to form CO_2 is through an ion exchange process facilitated by Alumina-Silica, which can form a zeolite structure [31]. However, the presence of Alumina-Silica in this sample is relatively low, so the CO reduction still needs to be improved. In addition, the diffusion factor significantly affects this process again due to the heterogeneous system. Meanwhile, The CO_2 adsorption process by CaO will depend on the diffusion process with hot gas pressure from the engine, where at the beginning of contact, CO_2 will only react with the CaO surface until it is saturated to form a layer of $CaCO_3$ (carbonization reaction) which is exothermic and spontaneous. However, this process will not stop because, considering that CaO is a mesoporous material, internal diffusion will occur in all of CaO. Therefore, although the second process is relatively slower, the reaction area will likely be much larger [32].

On the other hand, HC is an acidic compound, allowing the ccompounds to easily bond to the surface of the adsorbent. Furthermore, it was discovered that increasing the length of the catalytic converter further reduces the concentration of all pollutants. As a result, the longest adsorbent of 150 mm is the most effective in reducing emission concentrations. The longer the size of the adsorbent, the longer the contact duration between the engine emission and the adsorbent. Therefore, the longer the contact duration between engine emission and adsorbent results in a greater reduction in engine emission concentration. This condition increases the amount of reduced and oxidized engine emissions in the adsorbent, resulting in a significant emission reduction recorded by the engine emission analyser. In this study, the largest emission reduction occurred in CO_2, respectively 58.2% (adsorbent 150 mm), 30.6% (adsorbent 100 mm), and 0.4% (adsorbent 50 mm). A similar reduction pattern was also experienced for the other two emissions where the maximum reduction occurred at the adsorbent length of 150 mm, namely 49.9% and 57.1% respectively for CO and HC. The emission reduction recorded on the 150 mm adsorbent is very promising because it can reduce the emission concentration by half. These advantages provide information that CCR has the potential to be a good adsorbent, although it still depends on its size. Similarly, from the results obtained that the rate of high adsorption capacity occurs in the early minutes of the adsorption process. The adsorption capacity is effective in the early minutes because the adsorption process is dominated by a physical mechanism in which the pores that were originally open and ready to receive compounds have been filled with exhaust gas compounds. The pores become saturated over time, reducing the adsorbent's adsorption capacity.

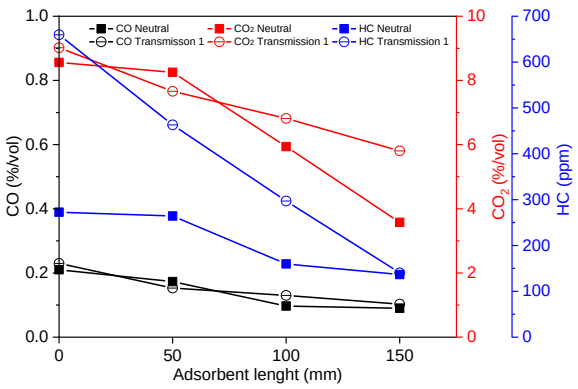

Figure 2. Engine exhaust gas emissions

When evaluating variations in different engine operating conditions, the emission concentration in the first transmission operating conditions shows a larger volume than the neutral transmission. The increase in engine load causes an increase in fuel supply into combustion chamber leading to an increase in engine emissions.

Figure 3 depicts the temperature distribution along the adsorbent and the exhaust gas line. This temperature profile displays measurement data commencing when the engine is started and continuing until the oil temperature constant. The temperature profile increases as the adsorbent length increases, both at idle and in the first engine

transmission. High temperatures were observed at all temperature measurement points from T1 to T7 both on the front and inside the adsorbent. The recorded high temperature is due to its proximity to the heat source. It is noticed that T3 decreased even though its position was in front of the adsorbent. This is due to an increase in cross-sectional area at the location of the temperature measurement. As a result, there is heat distribution accompanied by even temperature distribution on the cross section, resulting in a decrease in recorded temperature. Moreover, temperature gradually decreases as the location steps away from the heat source. Meanwhile, the measured high temperature on the longer adsorbent is due to the turbulence of the exhaust gas emission occurring at the front and inside the adsorbent. Turbulence occurs when the flow of exhaust gas emissions hits the adsorbent is obstructed, and the intensity of turbulence increases as the adsorbent's size increases. The greater the adsorbent, the greater the change in flow velocity and pressure. The obstruction of the exhaust gas flow due to hitting the adsorbent causes friction between the exhaust gas molecules to increase and leads to a large drag force. The existence of this drag causes the energy needed to move the exhaust gases to increase [33]. This causes the difference in exhaust gas pressure at the front and back of the adsorbent to increase.

The heat adsorbed by the calcium carbide adsorbent also causes an increase in temperature within the adsorbent. The larger the adsorbent, the more molecules that make up the CCR. Therefore, the greater the heat adsorption capacity by the CCR molecules leads to an increase in the average temperature of the adsorbent (see **Figure 3**). This is also supported by the relatively large molar heat capacity of calcium carbide [34]. According to this, the heat energy stored in the adsorbent is proportional to its cross-sectional area. Furthermore, due to the turbulence, exhaust gas emissions have a longer residence time in the adsorbent. Then, in conjunction with a high adsorbent temperature, it facilitates a better oxidation process of exhaust gas emissions, lowering emission concentrations.

The recorded pressure profiles for various variations in engine transmission and adsorbent length are depicted in **Figure 4**. It can be observed that the pressure differential between the inlet and outlet of the adsorbent (P1 and P2 respectively) is increasing in accordance with the adsorbent's size.

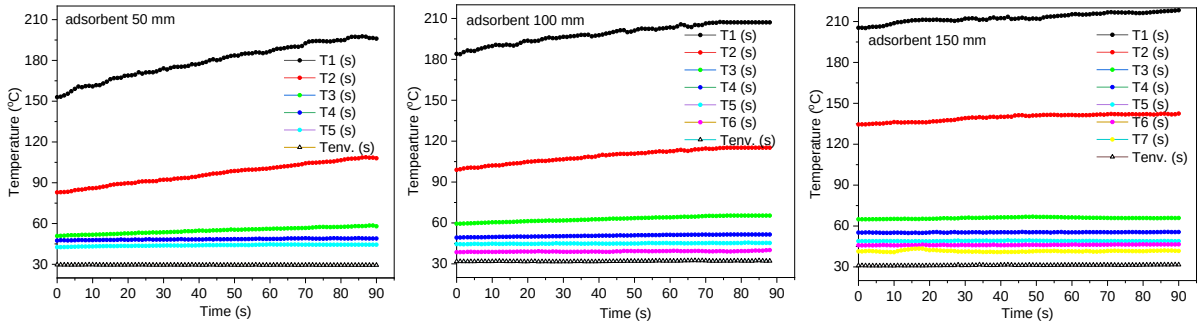

Figure 3. Temperature distribution over various dimensional adsorbents

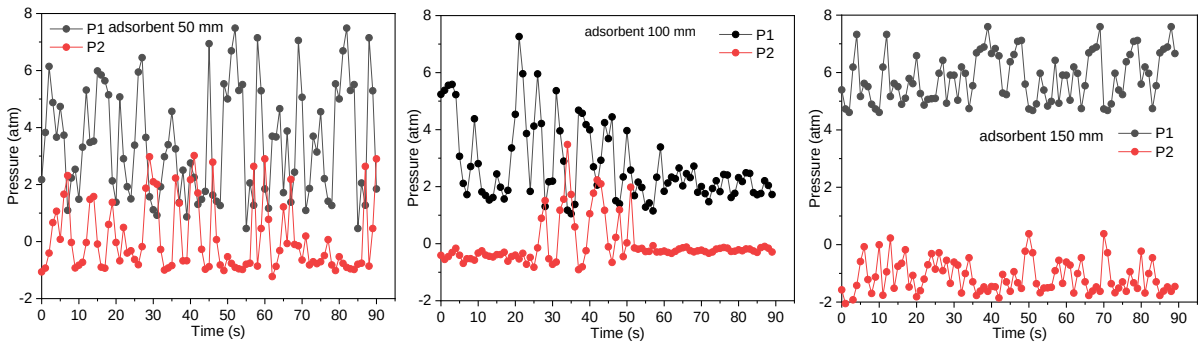

Figure 4. Pressure distribution over various dimensional adsorbents

The considerable pressure differential indicates that the exhaust emission turbulence is significant. The bigger the dimension of the adsorbent, the greater the pressure loss since it takes longer for the engine emissions to flow through the adsorbent, resulting in a pressure drop. This considerable pressure differential implies that exhaust emissions interaction with the adsorbent is at its maximum, leading the adsorbent to adsorb or oxidize more emissions.

3.2. *Adsorbent Performance Test*

The performance test of the CCR adsorbent unit was applied to a 150 mm adsorbent for four hours. The goal is to determine the adsorbent performance in lowering emissions after prolonged exposure to engine emissions. Based on emission testing, the adsorbent length of 150 mm showed the best emission adsorption among the other two adsorbents. This encourages further investigation to determine the degree to which the adsorbent can reduce exhaust emissions. Furthermore, the observation was carried out for four hours because the recorded emission concentrations had shown a constant trend and even began to increase, especially CO, which indicated that the adsorbent was getting saturated.

The results of the engine emission measurements presented in **Figure 5** reveal that the emission concentration fluctuates during engine operation for 240 minutes. However, it appears that CO and CO_2 levels are rising overall. This is primarily due to the decreasing efficacy of the adsorbent for adsorbing emissions. Observations showed that CO increased in concentration by 15.2% after four hours. On the other hand, HC and CO concentrations steadily declined, albeit at a slower rate. HC and CO decreased by 37.2% and 19.6%, respectively. The decrease in adsorption capacity occurs as the pores and channels of the adsorbent become saturated due to exhaust gas compounds.

Furthermore, fluctuations in emission data results are thought to be due to the fact that the amount of air and fuel mixture involved in the combustion chamber is not constant at each phase of the combustion process. This is owing to a high coefficient of performance (COV), which was not measured in this investigation. This is possible since the two-wheeler utilized still employs carburetors.

According to the pressure distribution measurement data, the pressure differential between P1 and P2 is increasing. It is hypothesized that after four hours, engine emissions adsorbed in the pores and adsorbent channels agglomerate and partially clog the holes. This indicates that the amount of exhaust gas emissions in the adsorbent has increased. On the other hand, HC is demonstrating a distinct trend, which is declining. This is most likely due to a rise in adsorbent temperature (see **Figure 3**), which resulted in a decrease in HC. The increase in adsorbent temperature resulted in more oxidized HC emissions, resulting in a decrease in HC content.

3.3. *Chemical Composition of CCR Adsorbent*

The results of the chemical composition analysis of CCR adsorbent are shown in **Table 4**.

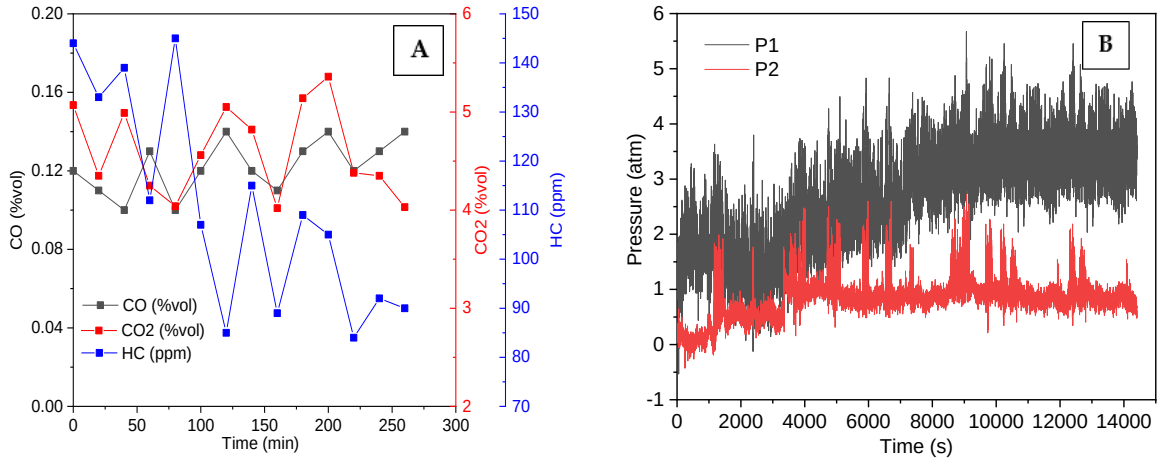

Figure 5. 150 mm length adsorbent performance test, A. engine exhaust gas emissions, B. pressure distribution

Table 4. Chemical composition of calcium carbide adsorbent

Sample	Substances	Compositions (% mass)
Adsorbent before contact with emissions	C	15.40
	Al_2O_3	5.36
	SiO_2	3.60
	SO_3	7.85
	CaO	67.79
Adsorbent after contact with emissions	C	18.11
	Al_2O_3	1.20
	SiO_2	2.52
	SO_3	1.87
	CaO	73.13
	ZrO_2	3.17

According to **Table 4**, there is an alteration in the chemical composition of the adsorbent after interaction with exhaust gas emissions. The results demonstrate that CaO compounds are the main constituents of calcium carbide and are becoming more prevalent as a result of exposure to exhaust gas emissions. Carbon atom also increased significantly by 17.6 %. Some compounds, however, exhibit a reduction in concentration after getting into contact with the emission. However, the decrease in these compounds resulted in an increase in the Si/Al ratio. This implies that the adsorbent adsorption capability is quite reliable. The presence of ZrO_2 was also detected in the adsorbent after contact with the emission. ZrO_2 is very commonly used as a catalyst component for exhaust emission converters and has a vital role in increasing the selectivity and effectiveness of the catalyst [35]. However, in this study, the built-in two-wheeler catalyst was removed. Therefore, the presence of ZrO_2 is most likely due to the oxides remaining in the exhaust manifold and being discharged into the environment as a pollutant.

The surface morphology of the sample was determined via SEM analysis. SEM analysis is a technique that uses electrons as an image source and an electromagnetic field as a lens. The image below depicts the findings of the adsorbent SEM examination.

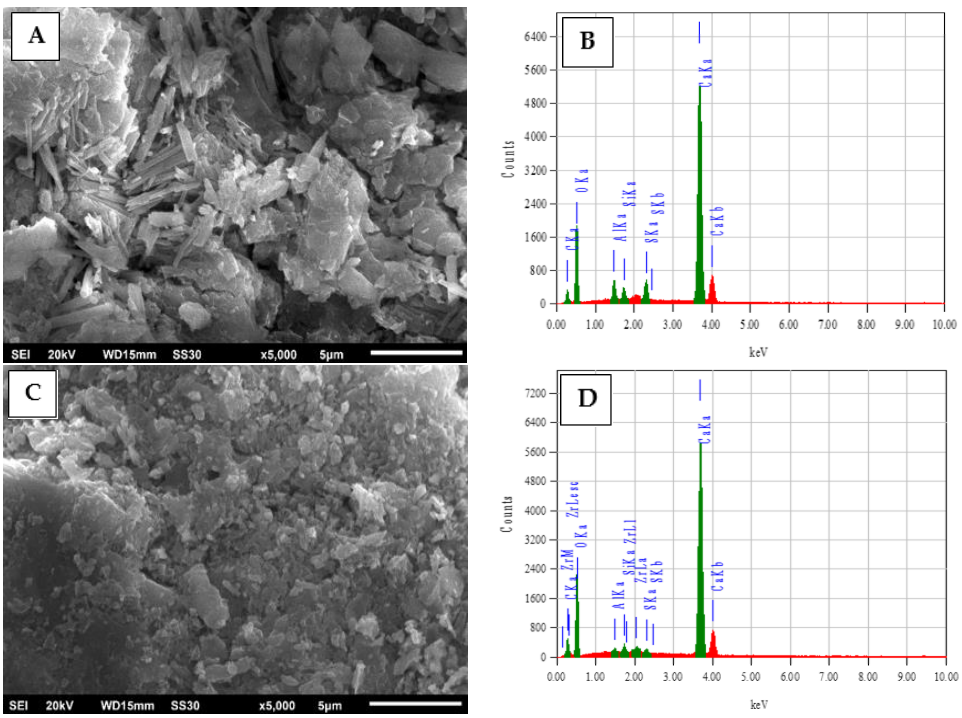

Figure 6. SEM and EDX results of calcium carbide adsorbent (A. SEM of adsorbent before contact with emissions, B. EDX of adsorbent before contact with emissions, C. SEM of adsorbent after contact with emissions, D. EDX of adsorbent after contact with emissions)

The surface morphology image of the adsorbent before contact with the engine emissions shows a collection of irregular particles in the shape of a rectangle and agglomerates of inhomogeneous size (**Figure 6A**). Pores and channels are also evenly distributed across the adsorbent surface. This demonstrates that the adsorbent has the capability of physically adsorb unwanted compounds from biogas through physical methods.

Figure 6C depicts the surface morphology of carbide adsorbent after being passed by emissions. It was noticed a cluster of irregular particles in the shape of lumps that are not homogeneous and have fewer holes. Forms and structures that existed before being exposed to engine emissions have been destroyed and transformed. This physical modification reduces the volume of pores and channels accessible to the adsorbent. The heat generated during the adsorption process is most likely responsible for this change in physical form. The adsorbent's high temperature and exhaust gas flow both contribute to the destruction of the adsorbent structure. This suggests that the adsorbent manufacturing process should be improved in order to obtain a tough adsorbent. The morphology change is also caused by the exhaust gas oxidation process, which occurs after the adsorbent has been saturated with exhaust gas compounds.

Electron Dispersive X-ray spectroscopy (EDX) is an analytical technique used to determine the elemental or chemical properties of specimens. The purpose of this analysis is to ascertain the chemical composition and various constituents of the specimen [36]. It was noted that carbon and calcium oxide increased significantly after interaction between the exhaust gas emissions and the adsorbent (**Figure 6D**). As a result, other molecules and components, such as alumina, silica oxide, and sulfur trioxide, decrease. This is reasonable considering that the primary elements of the adsorbent are carbon and calcium which have been oxidized at high temperatures.

3.4. FT-IR Test Results

As an adsorbent, CCR is made up of existing chemical species. The main ones are CaO, $Ca(OH)_2$ as the reaction of CaO with water vapour, and the presence of $CaCO_3$, which is very likely due to contact with outside air during the research process. Therefore, little is expected from FT-IR measurements other than to confirm the existence of these chemical species. However, after the adsorbent is exposed to exhaust gases, adsorption exceeds the previous state at a wave number of around 870 cm-1. These changes can be ascertained to occur because of the increased presence of carbonate ions due to the association of CaO with CO_2. Moreover, exhaust gasses such as CO, CO_2 and CH, are gases that have bond vibrational energies that are comparable to infrared energy, especially anti-symmetries vibrations. The ability to adsorb and re-emit infrared rays from these molecules causes heat trapped on the earth's surface, called greenhouse gases. Therefore, this study of exhaust gasses adsorption involves measuring the FT-IR spectrum on the adsorbent used before and after contact with the exhaust gas. Changes in the adsorbent due to the association of exhaust gasses with the adsorbent physically and chemically can be seen by observing changes in features in the FT-IR spectrum. Due to contact with high temperature exhaust emissions, the intermolecular bonds of the CCR become weak. This weakened bond leads to a more reactive CCR molecule in adsorbing energy and reacting with exhaust gas compounds [37]. From **Figure 7**, it is noticed that the strong association of CO_2 gas with CaO forming bonds in the $CaCO_3$ molecule was observed at 870 cm^{-1}.

According to the FT-IR spectrum image (**Figure 7**), both the adsorbent before and after contact with the exhaust gas engine emissions have OH groups at nearly the same wave number. The OH group with a sharp peak is typical of ordinary CaO. However, the presence of the OH group in

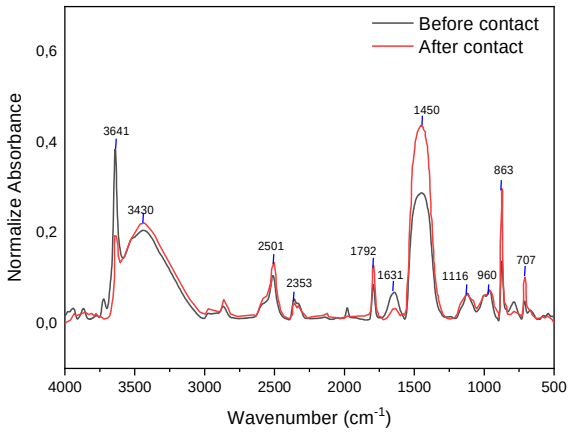

Figure 7. FT-IR results of calcium carbide adsorbent

area 3639.68 cm^{-1} to 3639.62 cm^{-1} cannot simply ensure that the analyzed sample is completely composed of CaO. This is due to the existence of an OH group in $Ca(OH)_2$ having a characteristic sharp peak in the area of 3643 cm^{-1}. As a result, these peaks could suggest the presence of water adsorbed on the CaO surface, where CaO is very easy to adsorb moisture from the air.

The carbonate group's C-O bending of carbonate ion vibration occurs naturally with a wave number of 870 cm^{-1}. In the sample before exposure to exhaust emission, the wave number occurs in the area of 873.75 cm^{-1}, which is close to the wave number in the sample after exposure to exhaust emissions, which is 873.70 cm^{-1}. The peak at the wave number of 870 cm^{-1} is a common feature of $CaCO_3$ and $Ca(OH)_2$. This suggests that the carbide sample used has a significant concentration of $CaCO_3$ and $Ca(OH)_2$ compounds. Overall, FT-IR results show insignificant feature changes both before and after contact time. This phenomenon is caused by adsorbate-adsorbent interactions that are dominated by physical interactions (Van der Walls) between the solid and gas phases. However, adsorption increased at wave numbers 1480 and 873 cm^{-1}. The Ca-O and carbonate ion vibrational regions are represented by the two peaks. This indicates that the oxide compound responsible for CO_2 adsorption is CaO oxide.

3.5. *Structure Characteristic of CCR*

Changes in the solid structure of the CCR were assessed by performing x-ray diffraction measurements (**Figure 8**) and comparing with JCPDS-ICDD cards. By observing the diffractogram, it is seen that there is a significant change in the crystal structure of the CCR before and after contact exhaust gasses. The initial adsorbent consist of CaO with peak lattice plane 53.88° (220) and 64.18° (311) with crystal cubic system (JCPDS No. 00-002-1088), also seen $Ca(OH)_2$ with peak lattice plane at 17.94° (001); 28.63° (100); 33.99°(101); 50.70°(110) and 62.46° (201) with hexagonal crystal system (JCPDS No. 01-084-1268). Therefore, not only the strong affinity of the chemical properties of this adsorbent, but the presence of cubic and hexagonal crystal structures in the material are very favourable for gas entrapment [38].

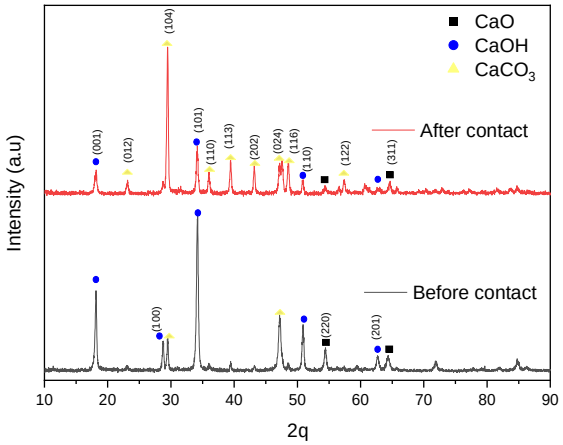

Figure 8. Diffractogram of CCR before (*black line*) and after (*red line*) contact with exhaust gasses

Structural changes on CCR after exposure to exhaust gasses were observed in the change in the diffractogram (red line), which was dominated by the peak of the central lattice plane of $CaCO_3$ at 23.14°(012); 29.55° (104); 39.49° (113); 47,30° (024) and 48,65° (116) with rhombohedral crystal system (JCPDS No.00-002-0629). This change indicates that there is not only a chemical bonding forming but also a transformation of the crystal form from a looser hexagonal structure to a denser rhombohedral structure (**Figure 9**). In addition, by using the Sharrer equation [38] we can approach the crystal size of the adsorbent and obtain an average crystal grain size of 29.24 nm. In other words, the material of this adsorbent has a large surface area, supporting the contact process with the flue gas. However, from the results of several tests, the CCR's ability to adsorb CO and CH gases has yet to be seen significantly. It is probably due to the lack of adsorbent affinity for the gas, so it is necessary to modify the composition of this adsorbent.

4. Conclusion

The results of the tests on the calcium carbide residue adsorbent reveal that the exhaust emissions of two-wheeler can be reduced by up to 58 percent in CO_2 and by almost the same amount in the other two emissions. This highest performance is attained on the adsorbent under a larger dimension of 150 mm. It was revealed that as the size of the adsorbent decreased, so did its ability. Furthermore, the adsorbent reduces exhaust pollutants through a physical adsorption mechanism. The benefit of having enough pores

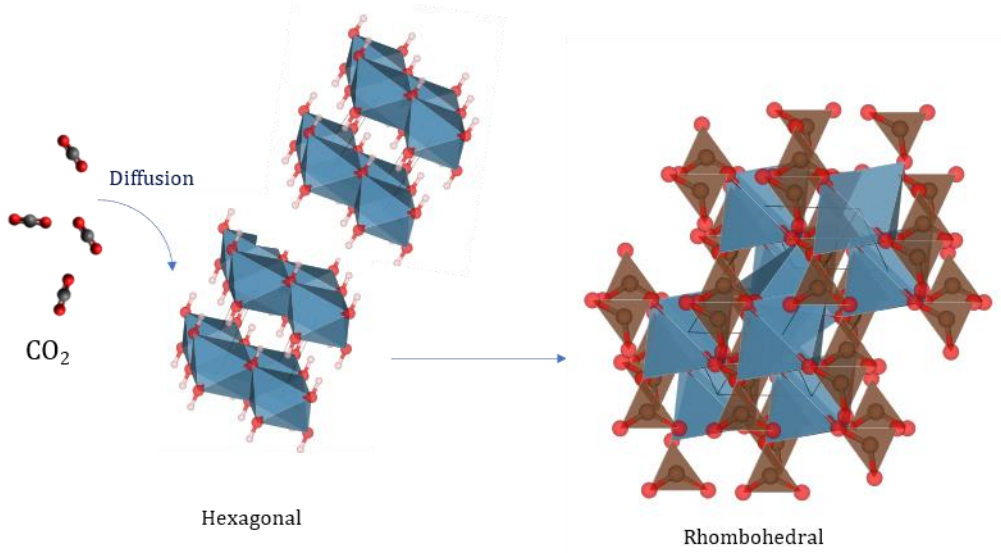

Figure 9. Transforming structure of solid state CCR from hexagonal to rhombohedral as consequence adsorbing CO_2 gas

and channels contributes to this favorable outcome. It is also supported by the adsorbent high temperature, particularly the adsorbent with bigger dimensions, which facilitates the oxidation process in reducing emissions. Observations of the adsorbent surface morphology revealed morphological alterations caused by high temperatures and gusts of exhaust gas emissions. The adsorption ability gradually declines as the effective adsorption surface area decreases. Based on 4-hour adsorbent durability test, it was discovered that engine emissions gradually increased, indicating that the adsorbent's efficiency was beginning to diminish.

Acknowledgement

The authors would like to thank the UPT Laboratorium Terpadu University of Diponegoro for providing the SEM, EDX, FT-IR and XRD data.

Author's Declaration

Authors' contributions and responsibilities

H. S. T., M.W., S.R.: The authors made substantial contributions to the conception and design of the study, The authors took responsibility for data analysis, interpretation and discussion of results and The authors read and approved the final manuscript; E.S., S.: The authors took responsibility for data analysis, interpretation and discussion of results and The authors read and approved the final manuscript.

Funding

This research did not receive any specific grant from funding agencies in the public, commercial, or not-for-profit sectors.

Availability of data and materials

All data are available from the authors.

Competing interests

The authors declare no competing interest.

Additional information

No additional information from the authors.

References

[1] F. B. Elehinafe, Y. J. Hassan, Q. E. Ebong-Bassey, and A. J. Adesanmi, "A Review on the Disposal Methods with Intrinsic Environmental and Economic Impacts of Scrap Tyres in Nigeria," *Automotive Experiences*, vol. 5, no. 2, pp. 103–110, 2022, doi: 10.31603/ae.5634.

[2] S. Sunaryo, P. A. Sesotyo, E. Saputra, and A. P. Sasmito, "Performance and Fuel Consumption of Diesel Engine Fueled by Diesel Fuel and Waste Plastic Oil Blends: An Experimental Investigation," *Automotive Experiences*, vol. 4, no. 1, pp. 20–26, 2021, doi: 10.31603/ae.3692.

[3] S. Mujiarto, B. Sudarmanta, H. Fansuri, and A. R. Saleh, "Comparative Study of Municipal Solid Waste Fuel and Refuse Derived Fuel in the Gasification Process Using Multi Stage Downdraft Gasifier," *Automotive Experiences*, vol. 4, no. 2, pp. 97–103, 2021, doi: 10.31603/ae.4625.

[4] M. A. Karim, S. Nasir, S. A. Rachman, and Novia, "Reduction of iron (II) ions in synthetic acidic wastewater containing ferro

sulphate using calcium carbide residu," *AIP Conference Proceedings*, vol. 2085, no. March, 2019, doi: 10.1063/1.5095003.

[5] W. Li and Y. Yi, "Use of carbide slag from acetylene industry for activation of ground granulated blast-furnace slag," *Construction and Building Materials*, vol. 238, p. 117713, 2020, doi: 10.1016/j.conbuildmat.2019.117713.

[6] P. Ramasamy, A. Periathamby, and S. Ibrahim, "Carbide sludge management in acetylene producing plants by using vacuum filtration," *Waste Management and Research*, vol. 20, no. 6, pp. 536–540, 2002, doi: 10.1177/0734242X0202000607.

[7] M. H. Al-Sayed, I. M. Madany, W. al-Khaja, and A. Darwish, "Properties of asphaltic paving mixes containing hydrated lime waste," *Waste Management & Research*, vol. 10, no. 2, pp. 183–194, 1992, doi: 10.1177/0734242X9201000206.

[8] T. Phoo-ngernkham *et al.*, "Low cost and sustainable repair material made from alkali-activated high-calcium fly ash with calcium carbide residue," *Construction and Building Materials*, vol. 247, p. 118543, 2020, doi: 10.1016/j.conbuildmat.2020.118543.

[9] N. Makaratat, C. Jaturapitakkul, C. Namarak, and V. Sata, "Effects of binder and CaCl2 contents on the strength of calcium carbide residue-fly ash concrete," *Cement and Concrete Composites*, vol. 33, no. 3, pp. 436–443, 2011, doi: 10.1016/j.cemconcomp.2010.12.004.

[10] S. Susanti, S. Nasir, H. Hermansyah, and A. Mataram, "Treatment of Wastewater from Rubber Industry Using Calcium Carbide Residue Adsorbent and Hybrid Membrane UF – RO," *Sriwijaya Journal of Environment*, vol. 4, no. 1, pp. 37–41, 2019, doi: 10.22135/sje.2019.4.1.37.

[11] L. Wu *et al.*, "Study on Preparation and Performance of Calcium Carbide Slag Foam for Coal Mine Disaster Reduction and CO2 Storage," *Colloids and Surfaces A: Physicochemical and Engineering Aspects*, vol. 606, no. July, p. 125322, 2020, doi: 10.1016/j.colsurfa.2020.125322.

[12] W. Li *et al.*, "Adsorptive Desulfurization of Diesel Oil by Alkynyl Carbon Materials Derived from Calcium Carbide and Polyhalohydrocarbons," *Energy and Fuels*, vol. 31, no. 9, pp. 9035–9042, 2017, doi: 10.1021/acs.energyfuels.7b01295.

[13] J. Saleem, U. Bin Shahid, M. Hijab, H. Mackey, and G. McKay, "Production and applications of activated carbons as adsorbents from olive stones," *Biomass Conversion and Biorefinery*, vol. 9, no. 4, pp. 775–802, 2019, doi: 10.1007/s13399-019-00473-7.

[14] S. K. Basha, N. V. Narasimha Rao, M. Shaik, and B. Stalin, "Performance analysis and control of NOx emissions in diesel engine using on-board acetylene gas from calcium carbide," *Materials Today: Proceedings*, vol. 33, no. xxxx, pp. 4887–4892, 2020, doi: 10.1016/j.matpr.2020.08.439.

[15] M. Anbia and Z. Parvin, "Desulfurization of fuels by means of a nanoporous carbon adsorbent," *Chemical Engineering Research and Design*, vol. 89, no. 6, pp. 641–647, 2011, doi: 10.1016/j.cherd.2010.09.014.

[16] P. Sakthivel, K. A. Subramanian, and R. Mathai, "Comparative studies on combustion, performance and emission characteristics of a two-wheeler with gasoline and 30% ethanol-gasoline blend using chassis dynamometer," *Applied Thermal Engineering*, vol. 146, pp. 726–737, 2019, doi: 10.1016/j.applthermaleng.2018.10.035.

[17] P. Sakthivel, K. A. Subramanian, and R. Mathai, "Experimental study on unregulated emission characteristics of a two-wheeler with ethanol-gasoline blends (E0 to E50)," *Fuel*, vol. 262, no. August 2019, p. 116504, 2020, doi: 10.1016/j.fuel.2019.116504.

[18] T. Mukesh, N. S.-R. J. of Engineering, and undefined 2012, "Reduction of Pollutant Emission from Two-wheeler Automobiles using Nano-particle as a Catalyst," *Academia.Edu*, vol. 1, no. 3, pp. 32–37, 2012.

[19] A. Granados-Pichardo, F. Granados-Correa, V. Sánchez-Mendieta, and H. Hernández-Mendoza, "New CaO-based adsorbents prepared by solution combustion and high-energy ball-milling processes for CO2 adsorption: Textural and structural influences," *Arabian Journal of Chemistry*, vol. 13, no. 1, pp. 171–183, 2020, doi: 10.1016/j.arabjc.2017.03.005.

[20] Y. Jung, Y. D. Pyo, J. Jang, G. C. Kim, C. P. Cho, and C. Yang, "NO, NO2 and N2O emissions over a SCR using DOC and DPF systems with Pt reduction," *Chemical Engineering Journal*, vol. 369, no. 2, pp. 1059–1067, 2019, doi: 10.1016/j.cej.2019.03.137.

[21] M. Mehregan and M. Moghiman, "Experimental investigation of the distinct effects of nanoparticles addition and urea-SCR after-treatment system on NOx emissions in a blended-biodiesel fueled internal combustion engine," *Fuel*, vol. 262, no. November, p. 116609, 2020, doi: 10.1016/j.fuel.2019.116609.

[22] O. Chiavola, G. Chiatti, and N. Sirhan, "Impact of particulate size during deep loading on DPF management," *Applied Sciences (Switzerland)*, vol. 9, no. 15, 2019, doi: 10.3390/app9153075.

[23] H. Chen *et al.*, "Entropy-stabilized metal oxide solid solutions as CO oxidation catalysts with high-temperature stability," *Journal of Materials Chemistry A*, vol. 6, no. 24, pp. 11129–11133, 2018, doi: 10.1039/c8ta01772g.

[24] S. Sinha Majumdar, J. A. Pihl, and T. J. Toops, "Reactivity of novel high-performance fuels on commercial three-way catalysts for control of emissions from spark-ignition engines," *Applied Energy*, vol. 255, p. 113640, 2019, doi: 10.1016/j.apenergy.2019.113640.

[25] R. Feng, X. Hu, G. Li, Z. Sun, and B. Deng, "A comparative investigation between particle oxidation catalyst (POC) and diesel particulate filter (DPF) coupling aftertreatment system on emission reduction of a non-road diesel engine," *Ecotoxicology and Environmental Safety*, vol. 238, no. June, pp. 1–34, 2022, doi: 10.1016/j.ecoenv.2022.113576.

[26] G. Wu *et al.*, "Cobalt oxide with flake-like morphology as efficient passive NOx adsorber," *Catalysis Communications*, vol. 149, no. October 2020, p. 106203, 2021, doi: 10.1016/j.catcom.2020.106203.

[27] A. Joshi and T. V. Johnson, "Gasoline Particulate Filters — a Review," *Emission Control Science and Technology*, vol. 4, no. 4, pp. 219–239, 2018, doi: 10.1007/s40825-018-0101-y.

[28] H. S. Tira *et al.*, "Influence of Fuel Properties, Hydrogen, and Reformate Additions on Diesel-Biogas Dual-Fueled Engine," *Journal of Energy Engineering*, vol. 140, no. 3, 2014, doi: 10.1061/(asce)ey.1943-7897.0000173.

[29] PT Pertamina, "Material Safety Data Sheet Premium RON 88 PT. Pertamina," in *PT Pertamina*, no. 2007, 2007, pp. 1–9.

[30] G. Senthilkumar, J. B. Sajin, D. Yuvarajan, and T. Arunkumar, "Evaluation of emission, performance and combustion characteristics of dual fuelled research diesel engine," *Environmental Technology (United Kingdom)*, vol. 41, no. 6, pp. 711–718, 2020, doi: 10.1080/09593330.2018.1509888.

[31] P. Wu *et al.*, "Cooperation of Ni and CaO at Interface for CO2 Reforming of CH4: A Combined Theoretical and Experimental Study," *ACS Catalysis*, vol. 9, no. 11, pp. 10060–10069, 2019, doi: 10.1021/acscatal.9b02286.

[32] J. A. Medrano *et al.*, "CO selective oxidation using catalytic zeolite membranes," *Chemical Engineering Journal*, vol. 351, no. December 2017, pp. 40–47, 2018, doi: 10.1016/j.cej.2018.06.084.

[33] M. J. Morrison and G. A. Kopp, "Effects of turbulence intensity and scale on surface pressure fluctuations on the roof of a low-rise building in the atmospheric boundary layer," *Journal of Wind Engineering and Industrial Aerodynamics*, vol. 183, no. October, pp. 140–151, 2018, doi: 10.1016/j.jweia.2018.10.017.

[34] X. K. Zhang, Z. X. Tong, D. Li, X. Hu, and Y. L. He, "Analysis and optimization about electromagnetics-temperature-component distribution in calcium carbide electric furnace," *Applied Thermal Engineering*, vol. 185, p. 115980, 2021, doi: 10.1016/j.applthermaleng.2020.115980.

[35] X. Li *et al.*, "Influence of ZrO2 crystal structure on the catalytic performance of Fe-Ni catalysts for CO2-assisted ethane dehydrogenation reaction," *Fuel*, vol. 322, no. August, pp. 15–17, 2022, doi: 10.1016/j.fuel.2022.124122.

[36] I. A. Abdalfattah, W. S. Mogawer, and K. Stuart, "Quantification of the degree of blending in hot-mix asphalt (HMA) with reclaimed asphalt pavement (RAP) using

Energy Dispersive X-Ray Spectroscopy (EDX) analysis," *Journal of Cleaner Production*, vol. 294, p. 126261, 2021, doi: 10.1016/j.jclepro.2021.126261.

[37] H. Y. Nanlohy, I. N. G. Wardana, N. Hamidi, L. Yuliati, and T. Ueda, "The effect of Rh3+ catalyst on the combustion characteristics of crude vegetable oil droplets," *Fuel*, vol. 220, pp. 220–232, 2018.

[38] A. Monshi, M. R. Foroughi, and M. R. Monshi, "Modified Scherrer Equation to Estimate More Accurately Nano-Crystallite Size Using XRD," *World Journal of Nano Science and Engineering*, vol. 02, no. 03, pp. 154–160, 2012, doi: 10.4236/wjnse.2012.23020.